TRANSPARENT AND EDIBLE FILMS FROM ULTRASOUND-TREATED EGG YOLK GRANULES

Ismael Marcet[1], Carlos Álvarez[2], Benjamín Paredes[1], Manuel Rendueles[1] & Mario Díaz[1,*]

1: Department of Chemical and Environmental Engineering, University of Oviedo, C/ Julián Clavería 8, 33006 Oviedo, Spain

2: Department of Food Chemistry, Teagasc Food Research Centre, Ashtown, Dublin 15, Ireland

* Corresponding author. Department of Chemical and Environmental Engineering, University of Oviedo, C/ Julián Clavería 8, 33006 Oviedo, Spain. Email: mariodiaz@uniovi.es

ABSTRACT

Whole egg yolk can be easily separated into two fractions, plasma and granules, the former of which is rich in lipids and the latter has a high protein content. Searching for new applications for each fraction could increase the value of the whole egg. In this work, the egg yolk granule fraction is being proposed and used to create transparent, edible films.

For that purpose, a solution of egg yolk granules was pre-treated using high intensity ultrasound. A Box-Behnken design was established to determine the effect of temperature, ultrasound intensity and the pre-treatment time on the clarity of the granules solution and the transparency of the films obtained. Furthermore, the films were analysed to test the effect of the ultrasound pre-treatment on their mechanical properties, solubility, colour, thermal stability and structure.

The optimal conditions for obtaining highly transparent films from egg yolk granules solution were found to be: 45 °C, for 40 minutes and applying ultrasounds at 60% amplitude. With this pre-treatment, the puncture strength value of the films improved from 9 N/mm, in the case of the untreated granules solution, to 31.6 N/mm. The puncture deformation showed a similar trend. All the films made with egg yolk granules showed a low water solubility. The colour of the films was not affected by the ultrasound pre-treatment.

Highlights:

- Yolk egg granules have been used to generate transparent edible films
- Optimum UT parameters were found to generate highly transparent films

- UT disrupted protein aggregates generating more homogeneous films
- Treated films showed enhanced mechanical properties

Keywords:

Edible films, egg yolk, response surface methodology, ultrasounds.

1. INTRODUCTION

The use of natural biopolymers as a source for producing packaging materials has been studied intensively in the last few years. These biopolymers have some desirable properties in comparison with polymers derived from petroleum. Specifically, these biopolymers are more easily recyclable, they come from a renewable and natural source, the environmental impact derived from their use and extraction is reduced and they can also be edible.

Films prepared from natural sources have been designed to be applied directly on the surface of the food product, forming a barrier which protects the packed product from the possible adverse effects of gases such as oxygen or water vapour and other undesirable substances. Among the desirable properties of these films are their organoleptic and mechanical properties, their stability over time, their non-contaminant properties, the simplicity of their preparation, and finally, their ability to be safely edible (Debeaufort et al. 1998). Transparency of the films is another key factor when they are intended to be applied as food coatings; due to the great impact on the final appearance of the product (Villalobos et al. 2005)

The preparation of these films varies according to the biopolymers used in their formulation. In the case of films made using proteins, the usual sources are gelatine (Cao et al. 2007; Ge et al. 2017; Fakhouri et al. 2018), whey protein (Galus and Kadzińska 2016; Marquez et al. 2017; Catarino et al. 2017), soya protein (Pan et al. 2014; Echeverría et al. 2017; Ortiz et al. 2017), egg proteins (Lim et al. 1998; Fuertes et al. 2017; Peng et al. 2017) and gluten (Tanada-Palmu and Grosso 2005; Sharma et al. 2017; Fakhouri et al. 2018). Usually, the preparation of these films requires the solubilization of the protein at different concentrations (w/v) in different solvents: such as water (A. Gennadios et al. 1996; Lim et al. 1998), a mix of water and ethanol (Tanada-Palmu and Grosso 2005) or another solvent (Qi et al. 2009). The use of a plasticizer is required to generate protein films. Glycerol has been used more extensively than others for this purpose (Vieira et al. 2011). Finally, the film-forming solution, which is composed of the solubilized protein and the plasticizer, is spread on a surface and dried to obtain the film (Umaraw and Verma 2015).

Egg yolk is composed of 50% dry matter, mainly lipids (62.5%) and proteins (33%) assembled in the form of lipoproteins (Huopalahti et al. 2007). This high lipid content, in comparison to that of proteins, prevents the formation of a consistent film and decreases the utility of the whole egg yolk for preparing packaging materials.

However, egg yolk can be easily separated into two fractions, the plasmatic and the granular. The former represents around 75-81% of total egg yolk solids (Le Denmat et al. 2000) and it is constituted mostly of low density lipoproteins (LDL) with high lipid content. This fraction is able to generate emulsions and gels similar to those obtained when whole yolk is employed (Le Denmat et al. 2000; M. Anton et al. 2001; Kiosseoglou and Paraskevopoulou 2005). After fractionation, the plasmatic fraction could be used directly as a food ingredient, harnessing in this way its excellent functional properties. However, few applications have been developed for the granular fraction. Thus, egg yolk fractionation, in spite of the advantages found in using the separated plasmatic fraction, is hard to justify at industrial level. The granular fraction is constituted mainly of high density lipoproteins (HDL). These HDLs provide 70% of the granular content (McCully et al. 1962) and they are in the form of aggregates along with other granular proteins, linked by means of phospho-calcium bonds. This fraction has a high protein content and low level of lipids in comparison with the whole egg yolk. In order to solubilize the proteins in this fraction a high ionic strength ≥ 0.3 M NaCl is required. Below this point, the granules from egg yolk show low solubility and therefore decreased functional properties, which limits their range of application. However, due to its high protein content, it is a potential source of material for producing edible films. The preparation of films using commercial gelatine combined with egg proteins has been recently reported (Fuertes et al. 2017). However, in this case, the films were generated with the assistance of the good film forming ability of the gelatine, since the granular fraction, which is practically insoluble, was not previously solubilized. In order to generate films composed merely of egg granular fraction proteins, a solubilization pre-treatment is required. Ultrasounds have been reported to increase protein solubility and functionality (Jambrak et al. 2008). However, the use of ultrasounds to favour the formation of protein-based edible films and to improve their properties has been scarcely studied. Banerjee et al. (1996) reported the effect of ultrasounds on the mechanical strength of milk protein-based films. Liu et al. (2004) found minor improvements in their ultrasound-treated peanut protein films. When high intensity ultrasounds are applied in a liquid, it produces cavitation due to the compression and decompression cycles of the sonic waves. As results, cavitation gas bubbles are generated, which then violently collapse resulting in high shearing effects. These shear forces and the energy inputs are strong enough to break non-covalent and covalent bonds of proteins

dissolved or in suspension in aqueous solutions (Gülseren et al. 2007).However, according to Banerjee et al. (1996), ultrasound treatment to improve films properties have to be optimised for each specific raw material.

In the present work, the solubilization of proteins recovered from egg yolk granules has been achieved by pH adjustment combined with ultrasounds and thermal treatment. The effect of ultrasounds on film properties has been characterised and optimised by means of RMS approach. As a result, a novel material has been obtained, which presents improved mechanical properties and enhanced transparency. Additionally, the use of gelatine is no longer required to obtain the films.

2. MATERIAL AND METHODS

2.1 Materials

Medium size eggs (50-60 g), were purchased from a local market ("Alimerka" placed in Oviedo, Spain). The following reagents were purchased in Sigma-Aldrich (St Louis, USA): sodium hydroxide (ref. 71687), glycerol (ref. G9012), Nile blue A (ref. N0766).

2.2 Egg yolk granules

Following the method of Laca et al. (2010), egg yolk and albumen were separated manually and the residual albumen was eliminated from the yolk employing blotting paper. Egg yolk material was mixed with water (1:1.5 v/v) and the pH of the diluted egg yolk was adjusted to 7 using NaOH (1 N). It was kept overnight at 4 °C and centrifuged at 10000 x g for 45 min to separate it into plasma (supernatant) and granules (sediment) fractions. Egg yolk granules were lyophilized and stored at -20 °C until used.

2.3 Film preparation

The results of preliminary studies indicated that the concentration of lyophilized granules used in the film-forming solution should be 3% (w/v, in ultrapure water). The lyophilized granules were gently stirred for 10 minutes using a magnetic stirring. The pH of the suspension was adjusted to a pH value of 9.5 by adding 850 µL of NaOH (1 M) for each 100 mL of granules solution. Twenty mL of this solution was treated with ultrasound using a Sonopuls HD 2070

system (Bandelin, Germany), equipped with an MS 73 probe, at a frequency of 20 kHz and testing several sonication amplitudes (100% amplitude equivalent to 212 µm). During the ultrasound process, the temperature in the sample was maintained constant using a water bath. Several reaction temperatures and times were tested (Table 1). Finally, glycerol was added at 40% (w/w) of the total dry matter content and 18 mL of the film forming solution was cast in Petri dishes (8.5 cm diameter). This solution was dried in an oven at 45 °C for 12-14 h. The films obtained were peeled entirely and analysed.

2.4 Experimental design

A response surface method was used to describe the effect of the reaction temperature (X_1), the reaction time (X_2), and the percentage of amplitude (X_3) on the transparency of both the film-forming solution and the films obtained. All the films obtained in this experimental design were detached entirely after the drying of the film-forming solution. Such parameters, and their ranges, were identified as being key variables based on previous studies performed in our laboratory. Accordingly, a Box-Behnken design (BBD) with three independent variables at three levels was created. Each independent variable was coded at three levels (-1, 0, +1), the coded and real values are shown in Table 1. A second-order model equation was used for this model, represented by equation (1). Box-Behnken (Box and Behnken 1960) was specifically selected rather than the central composite design, because it is more efficient and it requires fewer runs. Furthermore, the cubic form of the BBD includes experimental runs under conditions which fall in the midpoints of the border of the experimental design, avoiding the corners which represent combined factor extremes. Finally, the composite central design includes axial points outside the limits of the experimental cube which might be unsafe for the integrity of the ultrasound system. The software used for the design was Minitab 17 (Minitab Inc, Pennsylvania, USA).

$$Y = \beta_0 + \sum_{i=1}^{2} \beta_i X_i + \sum_{i=1}^{3} \beta_{ii} X_i^2 + \sum_{i=1}^{2} \sum_{j=i+1}^{3} \beta_{ij} X_i X_j \qquad (1)$$

where Y is the response variable and β_0, β_i, β_{ij} and β_{ij} are the intercept, linear, quadratic and interaction coefficients, respectively; X_i and X_j are independent variables.

2.4.1 Granule solution clarity, film thickness and film transparency

Clarity measurement techniques were adapted from Santhirasegaram et al. (2013). The transmittance of egg granule solutions at 660 nm was measured using a spectrophotometer (Helios gamma, thermo scientific, USA). A blank with distilled water was used as the reference in each case. The clarity was calculated as a percentage, the transmittance at 660 nm of the water was considered as 100% clarity.

Film thickness was measured using a micrometer (Mitutoyo Co., Japan) with an accuracy of ± 1 µm. Nine measurements were taken at different random locations of each film and the average values were calculated. Film transparency was determined according to the method described by Pérez et al. (2016). Briefly, the film transparency was tested using a spectrophotometer and measuring the light transmission at 600 nm of rectangular pieces of films. These films were directly placed in the spectrophotometer test cell. An empty test cell was used as the blank. The transparency was calculated as a percentage, the transmittance of the blank at 600 nm was considered 100% of transparency.

2.5 Granule solution particle size measurement

2.5.1 Fluorescence microscopy

Granules solutions were stained using Nile blue A (0.01%), adding 3 mL of stain to 2 mL of sample. Fifty µL of sample was placed on a microscope slide and a cover slip was used to create a thin layer of preparation. Micrographs with 10x magnification of the granules solutions were obtained using an Olympus BX50 equipped with a fluorescence filter cube U-MNB2 (Olympus, Japan). The fluorophore in the samples was excited using a wavelength in the range of 470-490 nm. The emission wavelength detected started at 520 nm. The number and size of the particles was calculated using the ImageJ software.

2.5.2 Dinamic light scattering

The average size of the particles contained in the egg yolk granule solution was measured using dynamic light scattering (Zetasizer, UK). The Z-Average (nm) and the polydispersity index (PDI) values were measured in each case.

2.6 Film characterization

Prior to testing, all films were conditioned for 2 days at 21 °C and 54 ± 2% RH in a closed chamber which contained a saturated $Mg(NO_3)_2$ solution.

2.6.1 Mechanical properties of the film

The puncture strength (PS) and puncture deformation (PD) at the breaking point of the films were determined by means of puncture test (Otero-Pazos et al. 2016; Sobral et al. 2001; Blanco-Fernandez et al. 2013). These mechanical properties were analysed employing a TA.XT.plus Texture Analyser (Stable Microsystems, UK), using a 5 kg load cell and a 5 mm diameter probe (P/5S). The films were cut into strips of 15x20 mm. Then the sample film was placed between the two plates which form part of the tension grip system, and the plates were firmly screwed to the analyser. These plates have an orifice of 10 mm diameter which allows the probe to enter in contact with the film at a velocity of 1 mm/s, stretching the film until break. The PS and PD were calculated according to the following equations:

$$\mathrm{PS} = \mathrm{Fm}/\mathrm{Th} \qquad (2)$$

$$\mathrm{PD} = \left(\sqrt{\mathrm{D}^2 + \mathrm{R}^2} - \mathrm{R}\right)/\mathrm{R} \qquad (3)$$

Where Fm is the maximum force applied before the film rupture and Th is the film thickness; D is the distance covered by the probe while it is in contact with the film until the film is broken; R is the radio of the orifice in the plates.

2.6.2 Film solubility and water vapour permeability (WVP)

The solubility of the films was determined according to the method of Pérez-Mateos et al. (2009). Briefly, two circular pieces of film of 0.2 g were immersed in distilled water for 24 hours. Then the samples were filtered through Whatman no.1 paper filter, whose weight had been previously recorded, and dried at 105 °C for 12 hours. In a similar way, pieces of films that had not been immersed in water were directly dried to determine the dry matter of films. The water-soluble matter was calculated as the difference in weight before and after the water solubilization. The dry matter values obtained were measured using a halogen moisture analyzer (HR80, Mettler-Toledo, Switzerland).

The WVP was measured according to the ASTM standard Method E96-95 (1995) with the corrections proposed by Gennadios et al. (1994) to calculate the pressure of water vapour in the under surface film. A polyvinyl chloride based cup with a diameter of 6 cm and a depth of 8 cm

was filled with deionized water, leaving a gap of 1.5 cm between the surface of the water and the film under surface. The thickness of the film samples was measured in nine points. The mounted cups were placed inside an environmental chamber at 25 °C and 50 ± 2% RH and the weight loss was recorded each hour during the first 10 hours and finally after 24 h. Four replicates of each film were evaluated. The weight loss was plotted in function of time and the water vapour transmission rate (WVPR: gmol m^{-2} h^{-1}) was estimated by dividing the slope in the linear region (R^2 > 0.998) by the film surface. The WVP was calculated using the following equations:

$$P_{w1} = P_T - (P_T - P_{w0})\exp[(R \times T \times WVTR \times h)/(P_T \times D_{air})] \quad (4)$$

$$\Delta P = P_{w1} - P_{w2} \quad (5)$$

$$WVP = (WVTR \times Th)/\Delta P \quad (6)$$

Where P_{w1} is the corrected partial pressure of water at the underside film (Pa); P_T is the total atmospheric pressure (Pa); P_{w0} is partial pressure of water in the surface of the distilled water (Pa); R is universal gas constant (8,306,600 Pa cm^3 $gmol^{-1}$ K^{-1}); T is the test temperature (298 K); h is the height of the gap (cm); D_{air} is the diffusion coefficient of water vapour in air (cm^2 s^{-1}); ΔP is the real water vapour partial pressure difference across de film (Pa); Th is the thickness of the film (cm).

2.6.3 Film colour

A CIE Lab color scale was used to measure the degree of lightness (L), redness (+a) or greenness (-a), and yellowness (+b) or blueness (-b) of the films, using an UltraScan VIS spectrophotometer (HunterLab, USA). This spectrophotometer uses D65 illumination and 10^o observer. Films were measured on the surface of the white standard plate, which shows L*, a*, b* values of 97.12, -0.01 and 0.13 respectively. The total colour difference was calculated according to the following equation (Salgado et al. 2011):

$$\Delta E = \sqrt{(L_{film} - L_{control})^2 + (a_{film} - a_{control})^2 + (b_{film} - b_{control})^2} \quad (7)$$

2.6.4 Thermal properties

Thermo-gravimetric analyses were carried out using a TGA analyser SDTA851e (Mettler-Toledo, Switzerland) from 25 °C to 650 °C under a nitrogen atmosphere. The heating rate was 10 °C/min.

2.6.5 Scanning electron microscopy (SEM)

The micrographs of the film cross-section were carried out according to Kadam et al. (2015) and using a scanning electron microscope (SEM) (JSM-6610LV, JEOL, USA). To obtain the microstructure of the cross-section, film samples were cut into squares of 1x1 cm using a surgical blade. The film squares were mounted around stubs perpendicularly coated with gold. The magnification used was 450x, and the voltage was set at 5 kV.

2.7 Statistical analysis

Analysis of variance (ANOVA) was applied. Least significant differences (LSD) were calculated by Fisher's test to determine significant differences between the tested samples. These analyses were performed using the statistical software Statgraphics® V.15.2.06.

3. RESULTS

3.1 Effect of ultrasound pre-treatment parameters on GSC and FT

In order to characterize the effect of the ultrasonic pre-treatment on the clarification of the granule solution (GSC) and on the films transparency (FT) obtained, a Box-Behnken design matrix including these parameters was created (Table 1). The runs presented in Table 1 were carried out randomly, but the results are shown ordered from the lowest to the highest film transparency values for a better understanding. When studying the film transparency, the film thickness has to be taken into account for the calculation of this parameter. However, as can be seen from Table 1, the thickness of the tested films was found not significantly different, thus it was not considered.

As it can be seen in Table 1, specific combinations of temperature, reaction time and sonication amplitude were able to achieve a remarkable increase in the clarity of the granule solution,

resulting in the production of films with a higher degree of transparency. Specifically, the highest granule solution clarity was obtained at the design points 13, 14 and 15, which also correspond with film transparency values higher than 94%. These experimental points are composed of different values of temperature, time and sonication amplitude, but in all these tested runs at least two of these independent variables were set with the coded value of 1. This suggests a linear relation between the response obtained and the variables. However, the operational temperature, time and sonication amplitude values were limited by the ultrasound system itself; upper limits were fixed according to the ultrasonic system specifications, and the need to avoid damage due to overheating. The use of the BBD avoids the need for runs to be carried out at the maximum values of these three independent variables together, thus lengthening the lifetime of the ultrasonic device. Nevertheless, in terms of film transparency, an excellent value was achieved.

The analysis of variance (ANOVA) obtained after fitting the experimental data to the second order polynomial model (1) is shown in Table 2. In Table 2 only the statistically significant parameters (p-value < 0.05) were considered. Furthermore, the coded values in the coefficient estimate column were used to measure the significance of the coefficients, since coded units allow compare the size of the coefficients on a common scale. In the case of the granule solution clarity, two interactions were significant: time and temperature of sonication (X_{12}) and temperature and sonication amplitude (X_{23}). This first interaction denotes that the effect of temperature was more relevant at high reaction times. Therefore, at 10 min, increments in the reaction temperature did not produce an increase in the evaluated response. However, at 40 min, increments in the temperature can produce noticeable changes in the granule solution clarity. The second interaction detected can be interpreted in a similar way. In this case an increase in the time of reaction produced greater changes in the response obtained at high sonication amplitudes. However, the effect of the time is not so pronounced at the lowest sonication amplitude tested. According to these results, the time of reaction is the most important independent variable tested. In fact, setting the other two variables at an appropriate level, small changes in the time can produce greater variations in the tested responses.

Regarding the linear terms and in agreement with the comments above, the most important parameter was X_2 (time of reaction), followed by X_1 (temperature of sonication) and X_3 (sonication amplitude). Compared to these parameters, the other shown in Table 2 (X_2^2, quadratic term of time of sonication) had a reduced effect, although it was still statistically significant.

The fitted model for the granules solution clarity is shown in the following equation:

$$\%\mathrm{GSC} = 7.4 - 0.429\mathrm{X}_1 - 1.538\mathrm{X}_2 - 0.147\mathrm{X}_3 + 0.027\,\mathrm{X}_2^2 + 0.052\mathrm{X}_1\mathrm{X}_2 + 0.033\mathrm{X}_2\mathrm{X}_3 \quad (8)$$

Where %GSC is the percentage of clarity in the granules solution; X_1: temperature; X_2: time; X_3: sonication amplitude; X_2^2 quadratic term of time of sonication; $\mathrm{X}_1\mathrm{X}_2$: interaction between the temperature and the time; $\mathrm{X}_2\mathrm{X}_3$: interaction between the time and the sonication amplitude.

This model shows a lack of fit which has an F and p-value of 7.51 and 0.122 respectively. While the F is not significant in comparison to the F calculated for the model, the p-value is higher than 0.05, these two statistical parameters indicating that the model represents the experimental data appropriately. Furthermore, the quality of the model was confirmed by the coefficient of determination (R^2=0.97), with a high value in the adjusted R^2 (0.96) analysis too.

Not only the analysis of variance of granule solution clarity, but also that of film transparency is shown in Table 2. The same interactions were found in this response: the interaction between time and temperature of sonication (X_{12}) and the interaction between temperature and sonication amplitude (X_{23}). These interactions can be explained in a similar way as in the case of the granules solution clarity. Furthermore, the linear variables had a greater effect on this response, and also with a similar order of importance (X_2>X_1>X_3). In general terms, the greatest difference between these dependent variables, with regard to the significant factors which appear in each model, was the inclusion of the quadratic term X_3^2 (p-value < 0.05) in the film transparency quadratic equation:

$$\%\mathrm{FT} = 99{,}700 - 0.088\mathrm{X}_1 - 0.351\mathrm{X}_2 - 1.313\mathrm{X}_3 - 0.012\mathrm{X}_2^2 + 0.014\mathrm{X}_3^2 + 0.016\mathrm{X}_1\mathrm{X}_2 + 0.012\mathrm{X}_2\mathrm{X}_3 \quad (9)$$

Where %FT is the percentage of film transparency; X_1: temperature; X_2: time; X_3: sonication amplitude; X_2^2 quadratic term of time of sonication; X_3^2 quadratic term of the sonication amplitude; $\mathrm{X}_1\mathrm{X}_2$: interaction between the temperature and the time; $\mathrm{X}_2\mathrm{X}_3$: interaction between the time and the sonication amplitude. Coefficients are expressed in uncoded units.

Regarding the lack of fit of the model shown in equation 9, it was characterized by a low F-value and a high p-value, both of them indicating a good fit of the experimental data to the quadratic equation obtained. The values for the R^2 and adjusted R^2 parameters were 0.97 and 0.96, respectively.

The two models described by equations 8 and 9 were used to generate the response surface plots shown in Figure 1. For that purpose and according to Table 1, one independent variable was fixed to the coded value of 0, while the others were varied within the range of study to describe the behaviour of the tested responses.

As shown in Figure 1 (a-c), the granule solution clarity increased with the increase in temperature, time and sonication amplitude; no plateau region was detected, which could suggest response saturation. It is likely that the testing of higher values for the independent variables than those included in this BBD would result in clearer granular solutions, but this option was discarded during the course of experimental design because of the technical limitations of the ultrasound system mentioned above. Furthermore, taking into account the film transparency values obtained (Figure 1, d-f), a greater clarity in the granules solution could hardly lead to higher values of film transparency, since for this response it was possible to reach values higher than 90%. Additionally, the similarity in shape between the response surface plots of granule solution clarity and film transparency is reasonably high, thus indicating that the increase in film transparency caused by ultrasound pre-treatment was due to the clarification of the granular solution.

Finally, it is worth pointing out that to obtain the highest values of clarity and transparency it was enough to increase two of the independent variables to their maximum values and maintain the other in within a medium range, regardless of what values were increased and which remained low. Therefore, in order to minimize the overheating of the sonic transducer system the parameters to obtain highly transparent films were set to 45 °C, which was the medium value tested; for 40 minutes and applying 60% of amplitude (127.2 µm); which correspond to the highest levels of these two variables. These values were selected to generate the granules solutions and the films for further characterization at different processing times.

3.2 Granule solution particle size measurement

Granules solutions were sonicated and samples were withdrawn at 10, 20, 30 and 40 min. A non-sonicated sample was used as control. Nile-blue A was used to stain lipid and protein-nature compounds, allowing their visualization by fluorescence microscopy (Kaewmanee et al. 2009). Figure 2 shown representative captions at each time of UT tested.

The presence of big-size particles, particularly observed in the control sample, could proceed from lipoproteins aggregates such LDLs, which supposes the 12% of the granular composition (Marc Anton 2007). After freeze-drying process LDLs vesicle-like structure is affected and become less soluble, thus generating a turbid solution. The spherical shapes observed in Figure 2 suggest either LDLs aggregation or flocculation phenomena after re-suspended.

As it is showed in Table 3, in the particle population column, 10 minutes of sonication were sufficient to produce a significant decreasing in the population of aggregates. Furthermore, at longer UT times (30 and 40 min) their number was significantly reduced ($P<0.05$) from 528 ± 60 to a final value lower than 2. The average particle area was also decreased due to the UT, which confirms the effect that ultrasounds have on the structure of these lipoproteins aggregates. Previous literature described how ultrasounds can disrupt protein aggregates leading to less turbid solutions. It has been reported that the reason for the observed decrease in the turbidity is due to disruption of non-covalent associative forces, such as hydrophobic and electrostatic interactions, and hydrogen bonds, which maintain protein aggregates in solution. The interactions disruptions are induced by high levels of hydrodynamic shear and turbulence due to ultrasonic cavitations. Thus, more aggressive ultrasound treatments lead to a higher degree of aggregates disruption, explaining the results observed in this work (Hu et al. 2013; Marcuzzo et al. 2010). Also at 30 and 40 minutes of UT, a magnification of 100x was attempted, but no additional aggregates were visible. When the samples were analysed using dynamic light scattering it was confirmed that the average size of the particles decreased with increasing UT times (Table 3). It leads to think that the mechanical stress caused by ultrasounds through the continuous generation and collapse of bubbles might lead to the disaggregation of these egg yolk clumps, resulting in a decrease in the degree of turbidity of the solution, and consequently, in more transparent films.

3.3 Mechanical properties of the film

As can be seen from Table 4, in the puncture strength (PS) and puncture deformation (PD) columns, the ultrasonic pre-treatment modified the mechanical properties of the films, which

became more resistant to mechanical stress and more flexible. The differences observed between the control and the samples obtained at different sonication times were significant ($P<0.05$); however, pre-treatments longer than 30 min seem to have a negligible effect on such film properties. These changes promoted by the ultrasound pre-treatment are related to the smaller average particle size and the reduced number of large particles observed. The increased molecular interactions due to the energy input could lead to higher molecular order and therefore increased film strength, which is in agreement with the results found in this work. This effect of higher molecular order can be observed as well in the SEM images. These observations are in agreement with Guilbert et al. (1995). Samples treated with ultrasounds for 30 minutes resulted very similar in its mechanical properties and particle size to those sonicated for 40 min. Aggregates formed could impede the formation of protein-protein interactions. So, once the aggregates have been broken down by means of UT more protein-protein interactions are established, leading to stronger and more flexible films.

3.4 Film colour

The egg yolk has a yellowish colour, mainly produced by the presence in its composition of fat-soluble carotenoids (Li-Chan and Kim 2008). Although most of the lipids are retained in the plasmatic fraction during the fractionation of the whole egg yolk, traces of these compounds can still be found in the granule fraction, and provide a yellowish colour to the films (Figure 3) and other products made with this high-protein content fraction (Laca et al. 2010; Marcet et al. 2015). When compared to the control, the ultrasound pre-treatment had no effect on the colour of the films, since no reduction in the b* parameter was observed (Table 4). Parameter ΔE is employed to describe how different two samples are in terms of colour; values higher than 3 mean colour differences appreciable to the naked eye. Values of ΔE were found to be lower than 3, which means that only trained observers can notice the colour difference between control and the different pre-treatments. Only control compared to the sample pre-treated with ultrasounds for 10 min ($\Delta E = 3.16$) resulted in differences noticeable to the naked eye.

3.5 Thickness, moisture content, water solubility and water vapour permeability

Film thickness, moisture content, water solubility and water vapour permeability are shown in Table 4. Taking into account that the different processing methods could have effect on the properties of the proteins (Del Hoyo et al. 2008), It was observed that ultrasound had a significant positive effect on the parameters evaluated at short pre-treatment times (10 min);

however, longer times (40 min) produced no significant changes ($P<0.05$). Particularly in the case of film thickness, a decreasing trend can be inferred, based on the mean values obtained, although no statistically significant differences for this parameter were found between the treated films. Furthermore, the untreated samples showed higher moisture content compared to the treated films, mainly due to the lower degree of packing of its granular components, as it was further confirmed by microscopy.

Water solubility is related to the water resistance, which is desirable to protect food products with a high humidity. In this case, all the tested samples showed low water solubility, due to the abovementioned fact that egg yolk granules are insoluble in distilled water and the aggregation of their proteins and lipoproteins during the film drying resulted in insoluble films.

It was not possible to evaluate the effect of UT on the WVP, since it was not possible to obtain control films of the required size for this analysis. Nevertheless, it was found that longer sonication times had no significant effect on this property. In comparison with other protein-based films found in the literature, these films were found to be between 3 and 9 times less permeable to water vapour than those made with whey protein isolate prepared with different plasticizers (Sobral et al. 2001), between 2 and 4 times less than those prepared with pea-protein and various glycerol concentrations (Choi and Han 2001), and similar to that made using soy protein isolate (1.7 g mm / m^2 h kPa) (Friesen et al. 2015). In these films made with the egg yolk granular fraction, the presence of lipids in their composition may have a positive effect on this property, as it did in the case of other protein-based films to which lipids were added (Avena-Bustillos and Krochta 1993; Rocca-Smith et al. 2016).

3.6 Thermal properties

TGA thermograms of the tested films are shown in Figure 4. Films thermal stability is a valuable characteristic of this type of packaging products; since low stability could narrow their range of applications. According to Figure 4, it is possible to distinguish two main stages of weight loss. The first stage can be observed in the temperature range 60-130 °C and it was associated with the loss of water from the film matrix (Su et al. 2010). The second stage was related to the thermal degradation of both proteins and glycerol, and it was more pronounced. This stage begins at temperatures between 170 and 180 °C, continuing with a high degree of weight loss between 300 and 500 °C. Similar behaviour was reported for other protein-based films (Nuthong

et al. 2009; Ramos et al. 2013). The residue obtained at 600 °C for all films tested was about 14% of the original weight, which is the expected result since all of them were prepared using the same film-forming solution composition.

According to Figure 4, a slight increase in thermal stability was found for the ultrasound-treated films, particularly if the film treated for 40 minutes is compared with the control. The highest differences were found in the range between 180 and 310 °C. This suggests the presence of agglomerations of heterogeneous material in the control films, resulting in a decomposition curve with two phases in comparison with the single decomposition curve observed for the films treated for 40 minutes.

3.7 Scanning electron microscopy

Micrographs of the transversal section of each film were taken (Figure 5). The cross section of the control film appeared thickened in comparison with the treated films. Furthermore, the untreated sample showed a heterogeneous structure, where it is possible to appreciate irregularities which could be interpreted as lipoprotein agglomerations. After 10 minutes of ultrasonic pre-treatment, film sections showed a more compact and homogeneous appearance; although, as can be appreciated in micrograph 5.b, the upper half was more homogeneous than the bottom half, meaning that the remaining aggregates were distributed near the bottom of the Petri dish while the film was drying. Extended UT pre-treatment produced an increment in the structural arrangement. In particular, the film treated for 40 minutes had a totally homogenous cross-section area. Finally, this structural improvement in the film matrix, caused by the disruption of the lipoprotein aggregates, probably led to the formation of a tighter network, and therefore the improvement in the film mechanical properties shown in section 3.3.

4. CONCLUSIONS

In this study is reported, for the first time, the production of edible films using only proteins from the egg yolk granular fraction and glycerol as a plasticizer. The optimum conditions for the ultrasound treatment, in order to generate more transparent films, were determined assisted by RSM approach. It was found that optimum ultrasound processing improved the clarity of the

casting solution, the mechanical properties, thickness and solubility of the films generated; while the colour, WVP properties and thermal behaviour of the films were not affected, regardless the ultrasonic treatment employed. Results observed (lower particle size, lower polidispersity index and higher film compaction), indicate that ultrasounds are able to disrupt the protein aggregates by modifying the protein structure, since non-covalent and covalent bond are broken down.

It has been demonstrated that ultrasounds have the potential to be used for film properties modification; allowing to generate good-quality films from new protein sources before non-used for this purpose.

REFERENCES

Anton, M. (2007). Composition and structure of hen egg yolk. In *Bioactive egg compounds* (pp. 1-6): Springer.

Anton, M., Le Denmat, M., Beaumal, V., & Pilet, P. (2001). Filler effects of oil droplets on the rheology of heat-set emulsion gels prepared with egg yolk and egg yolk fractions. *Colloids and Surfaces B: Biointerfaces, 21*(1–3), 137-147.

ASTM (1995). Standard test methods for water vapor transmission of materials. In A. b. o. A. standards (Ed.), *ASTM* (Vol. PA: ASTM E96-95, pp. 697-704). Philadelphia.

Avena-Bustillos, R., & Krochta, J. (1993). Water Vapor Permeability of Caseinate-Based Edible Films as Affected by pH, Calcium Crosslinking and Lipid Content. *Journal of Food Science, 58*(4), 904-907.

Banerjee, R., Chen, H., & Wu, J. (1996). Milk Protein-based Edible Film Mechanical Strength Changes due to Ultrasound Process. *Journal of Food Science, 61*(4), 824-828.

Blanco-Fernandez, B., Rial-Hermida, M. I., Alvarez-Lorenzo, C., & Concheiro, A. (2013). Edible chitosan/acetylated monoglyceride films for prolonged release of vitamin E and antioxidant activity. *Journal of applied polymer science, 129*(2), 626-635.

Box, G. E., & Behnken, D. W. (1960). Some new three level designs for the study of quantitative variables. *Technometrics, 2*(4), 455-475.

Cao, N., Fu, Y., & He, J. (2007). Preparation and physical properties of soy protein isolate and gelatin composite films. *Food Hydrocolloids, 21*(7), 1153-1162.

Catarino, M. D., Alves-Silva, J. M., Fernandes, R. P., Gonçalves, M. J., Salgueiro, L. R., Henriques, M. F., et al. (2017). Development and performance of whey protein active coatings with

Origanum virens essential oils in the quality and shelf life improvement of processed meat products. *Food Control, 80*, 273-280.

Choi, W. S., & Han, J. H. (2001). Physical and Mechanical Properties of Pea-Protein-based Edible Films. *Journal of Food Science, 66*(2), 319-322.

Debeaufort, F., Quezada-Gallo, J.-A., & Voilley, A. (1998). Edible films and coatings: tomorrow's packagings: a review. *Critical Reviews in Food Science, 38*(4), 299-313.

Del Hoyo, P., Rendueles, M., & Díaz, M. (2008). Effect of processing on functional properties of animal blood plasma. *Meat science, 78*(4), 522-528.

Echeverría, I., López-Caballero, M. E., Gómez-Guillén, M. C., Mauri, A. N., & Montero, M. P. (2017). Active nanocomposite films based on soy proteins-montmorillonite-clove essential oil for the preservation of refrigerated bluefin tuna (Thunnus thynnus) fillets. *International journal of food microbiology*.

Fakhouri, F. M., Martelli, S. M., Caon, T., Velasco, J. I., Buontempo, R. C., Bilck, A. P., et al. (2018). The effect of fatty acids on the physicochemical properties of edible films composed of gelatin and gluten proteins. *LWT-Food Science and Technology, 87*, 293-300.

Friesen, K., Chang, C., & Nickerson, M. (2015). Incorporation of phenolic compounds, rutin and epicatechin, into soy protein isolate films: mechanical, barrier and cross-linking properties. *Food Chemistry, 172*, 18-23.

Fuertes, S., Laca, A., Oulego, P., Paredes, B., Rendueles, M., & Díaz, M. (2017). Development and characterization of egg yolk and egg yolk fractions edible films. *Food Hydrocolloids, 70*, 229-239.

Galus, S., & Kadzińska, J. (2016). Whey protein edible films modified with almond and walnut oils. *Food Hydrocolloids, 52*, 78-86.

Ge, L., Zhu, M., Xu, Y., Li, X., Li, D., & Mu, C. (2017). Development of Antimicrobial and Controlled Biodegradable Gelatin-Based Edible Films Containing Nisin and Amino-Functionalized Montmorillonite. *Food and Bioprocess Technology, 10*(9), 1727-1736.

Gennadios, A., Weller, C. L., & Gooding, C. H. (1994). Measurement errors in water vapor permeability of highly permeable, hydrophilic edible films. *Journal of Food Engineering, 21*(4), 395-409.

Gennadios, A., Weller, C. L., Hanna, M. A., & Froning, G. W. (1996). Mechanical and Barrier Properties of Egg Albumen Films. *Journal of Food Science, 61*(3), 585-589.

Guilbert, S., Gontard, N., & Cuq, B. (1995). Technology and applications of edible protective films. *Packaging Technology and Science, 8*(6), 339-346.

Gülseren, İ., Güzey, D., Bruce, B. D., & Weiss, J. (2007). Structural and functional changes in ultrasonicated bovine serum albumin solutions. *Ultrasonics sonochemistry, 14*(2), 173-183.

Hu, H., Wu, J., Li-Chan, E. C., Zhu, L., Zhang, F., Xu, X., et al. (2013). Effects of ultrasound on structural and physical properties of soy protein isolate (SPI) dispersions. *Food Hydrocolloids, 30*(2), 647-655.

Huopalahti, R., López-Fandiño, R., Anton, M., & Schade, R. (2007). *Bioactive egg compounds*: Springer.

Jambrak, A. R., Mason, T. J., Lelas, V., Herceg, Z., & Herceg, I. L. (2008). Effect of ultrasound treatment on solubility and foaming properties of whey protein suspensions. *Journal of Food Engineering, 86*(2), 281-287.

Kadam, S. U., Pankaj, S. K., Tiwari, B. K., Cullen, P. J., & O'Donnell, C. P. (2015). Development of biopolymer-based gelatin and casein films incorporating brown seaweed *Ascophyllum nodosum* extract. *Food Packaging and Shelf Life, 6*, 68-74.

Kaewmanee, T., Benjakul, S., & Visessanguan, W. (2009). Changes in chemical composition, physical properties and microstructure of duck egg as influenced by salting. *Food Chemistry, 112*(3), 560-569.

Kiosseoglou, V., & Paraskevopoulou, A. (2005). Molecular interactions in gels prepared with egg yolk and its fractions. *Food Hydrocolloids, 19*(3), 527-532.

Laca, A., Sáenz, M., Paredes, B., & Díaz, M. (2010). Rheological properties, stability and sensory evaluation of low-cholesterol mayonnaises prepared using egg yolk granules as emulsifying agent. *Journal of Food Engineering, 97*(2), 243-252.

Le Denmat, M., Anton, M., & Beaumal, V. (2000). Characterisation of emulsion properties and of interface composition in O/W emulsions prepared with hen egg yolk, plasma and granules. *Food Hydrocolloids, 14*(6), 539-549.

Li-Chan, E. C., & Kim, H.-O. (2008). Structure and chemical composition of eggs. *Egg bioscience and biotechnology*, 1-96.

Lim, L.-T., Mine, Y., & Tung, M. A. (1998). Transglutaminase cross-linked egg white protein films: tensile properties and oxygen permeability. *Journal of Agricultural and Food Chemistry, 46*(10), 4022-4029.

Liu, C.-C., Tellez-Garay, A. M., & Castell-Perez, M. E. (2004). Physical and mechanical properties of peanut protein films. *LWT-Food Science and Technology, 37*(7), 731-738.

Marcet, I., Paredes, B., & Díaz, M. (2015). Egg yolk granules as low-cholesterol replacer of whole egg yolk in the preparation of gluten-free muffins. *LWT-Food Science and Technology, 62*(1), 613-619.

Marcuzzo, E., Peressini, D., Debeaufort, F., & Sensidoni, A. (2010). Effect of ultrasound treatment on properties of gluten-based film. *Innovative Food Science & Emerging Technologies, 11*(3), 451-457.

Marquez, G. R., Di Pierro, P., Mariniello, L., Esposito, M., Giosafatto, C. V., & Porta, R. (2017). Fresh-cut fruit and vegetable coatings by transglutaminase-crosslinked whey protein/pectin edible films. *LWT-Food Science and Technology, 75*, 124-130.

McCully, K., Mok, C.-C., & Common, R. (1962). Paper elegtrophoretic characterization of proteins and lipoproteins of hen's egg yolk. *Canadian Journal of Biochemistry and Physiology, 40*(7), 937-952.

Nuthong, P., Benjakul, S., & Prodpran, T. (2009). Characterization of porcine plasma protein-based films as affected by pretreatment and cross-linking agents. *International journal of biological macromolecules, 44*(2), 143-148.

Ortiz, C. M., de Moraes, J. O., Vicente, A. R., Laurindo, J. B., & Mauri, A. N. (2017). Scale-up of the production of soy (*Glycine max L.*) protein films using tape casting: Formulation of film-forming suspension and drying conditions. *Food Hydrocolloids, 66*, 110-117.

Otero-Pazos, P., Sendón, R., Blanco-Fernandez, B., Blanco-Dorado, S., Alvarez-Lorenzo, C., Concheiro, A., et al. (2016). Preparation of antioxidant active films based on chitosan: diffusivity study of α-tocopherol into food simulants. *Journal of Food Science and Technology*, 1-10.

Pan, H., Jiang, B., Chen, J., & Jin, Z. (2014). Blend-modification of soy protein/lauric acid edible films using polysaccharides. *Food Chemistry, 151*, 1-6.

Peng, N., Gu, L., Li, J., Chang, C., Li, X., Su, Y., et al. (2017). Films Based on Egg White Protein and Succinylated Casein Cross-Linked with Transglutaminase. *Food and Bioprocess Technology*, 1-9.

Pérez-Mateos, M., Montero, P., & Gómez-Guillén, M. (2009). Formulation and stability of biodegradable films made from cod gelatin and sunflower oil blends. *Food Hydrocolloids, 23*(1), 53-61.

Pérez, L. M., Piccirilli, G. N., Delorenzi, N. J., & Verdini, R. A. (2016). Effect of different combinations of glycerol and/or trehalose on physical and structural properties of whey protein concentrate-based edible films. *Food Hydrocolloids, 56*, 352-359.

Qi, Q.-l., Li, Q., Lu, J.-w., Guo, Z.-x., & Yu, J. (2009). Preparation and characterization of soluble eggshell membrane protein/chitosan blend films. *Chinese Journal of Polymer Science, 27*(03), 387-392.

Ramos, Ó. L., Reinas, I., Silva, S. I., Fernandes, J. C., Cerqueira, M. A., Pereira, R. N., et al. (2013). Effect of whey protein purity and glycerol content upon physical properties of edible films manufactured therefrom. *Food Hydrocolloids, 30*(1), 110-122.

Rocca-Smith, J. R., Marcuzzo, E., Karbowiak, T., Centa, J., Giacometti, M., Scapin, F., et al. (2016). Effect of lipid incorporation on functional properties of wheat gluten based edible films. *Journal of Cereal Science, 69*, 275-282, doi:https://doi.org/10.1016/j.jcs.2016.04.001.

Salgado, P. R., Fernández, G. B., Drago, S. R., & Mauri, A. N. (2011). Addition of bovine plasma hydrolysates improves the antioxidant properties of soybean and sunflower protein-based films. *Food Hydrocolloids, 25*(6), 1433-1440.

Santhirasegaram, V., Razali, Z., & Somasundram, C. (2013). Effects of thermal treatment and sonication on quality attributes of Chokanan mango (*Mangifera indica L.*) juice. *Ultrasonics sonochemistry, 20*(5), 1276-1282.

Sharma, N., Khatkar, B., Kaushik, R., Sharma, P., & Sharma, R. (2017). Isolation and development of wheat based gluten edible film and its physicochemical properties. *International Food Research Journal, 24*(1).

Sobral, P. J. A., Menegalli, F. C., Hubinger, M. D., & Roques, M. A. (2001). Mechanical, water vapor barrier and thermal properties of gelatin based edible films. *Food Hydrocolloids, 15*(4–6), 423-432.

Su, J.-F., Huang, Z., Yuan, X.-Y., Wang, X.-Y., & Li, M. (2010). Structure and properties of carboxymethyl cellulose/soy protein isolate blend edible films crosslinked by Maillard reactions. *Carbohydrate Polymers, 79*(1), 145-153.

Tanada-Palmu, P. S., & Grosso, C. R. F. (2005). Effect of edible wheat gluten-based films and coatings on refrigerated strawberry (Fragaria ananassa) quality. *Postharvest Biology and Technology, 36*(2), 199-208.

Umaraw, P., & Verma, A. K. (2015). Comprehensive Review on Application of Edible Film on Meat and Meat Products: An Eco-friendly Approach. *Critical Reviews in Food Science and Nutrition*, 00-00, doi:10.1080/10408398.2014.986563.

Vieira, M. G. A., da Silva, M. A., dos Santos, L. O., & Beppu, M. M. (2011). Natural-based plasticizers and biopolymer films: A review. *European Polymer Journal, 47*(3), 254-263.

Villalobos, R., Chanona, J., Hernández, P., Gutiérrez, G., & Chiralt, A. (2005). Gloss and transparency of hydroxypropyl methylcellulose films containing surfactants as affected by their microstructure. *Food Hydrocolloids, 19*(1), 53-61.

Figure 1. Response surfaces for the clarity of the granule solution (GSC (%)) and for film transparency (FT (%)). GSC (%) response observed in relation with the reaction temperature and time (a), sonication amplitude and reaction temperature (b), and sonication amplitude and reaction time (c). FT (%) response observed in relation with the reaction temperature and time (d), sonication amplitude and reaction temperature (e), and sonication amplitude and reaction time (f).

Figure 2. Fluorescence microscopic image captions (10x magnification) treated using imageJ software. a) Granules solution control, no UT. b) Granules solution 10 min UT. c) Granules solution 20 min UT. d) Image caption representative of the granules solutions UT for 30 and 40 min.

Figure 3. The appearance of the films. Control (A), 10 min (B), 20 min (C), 30 min (D) and 40 min (E) of ultrasounds pre-treatment.

Figure 4. TGA curves of films made with ultrasound treated granules solutions.

Figure 5. Effect of ultrasound pre-treatment on the films cross-section area. a) control; b, c, d, e) 10, 20, 30 and 40 minutes of pre-treatment respectively.

Figure 1.

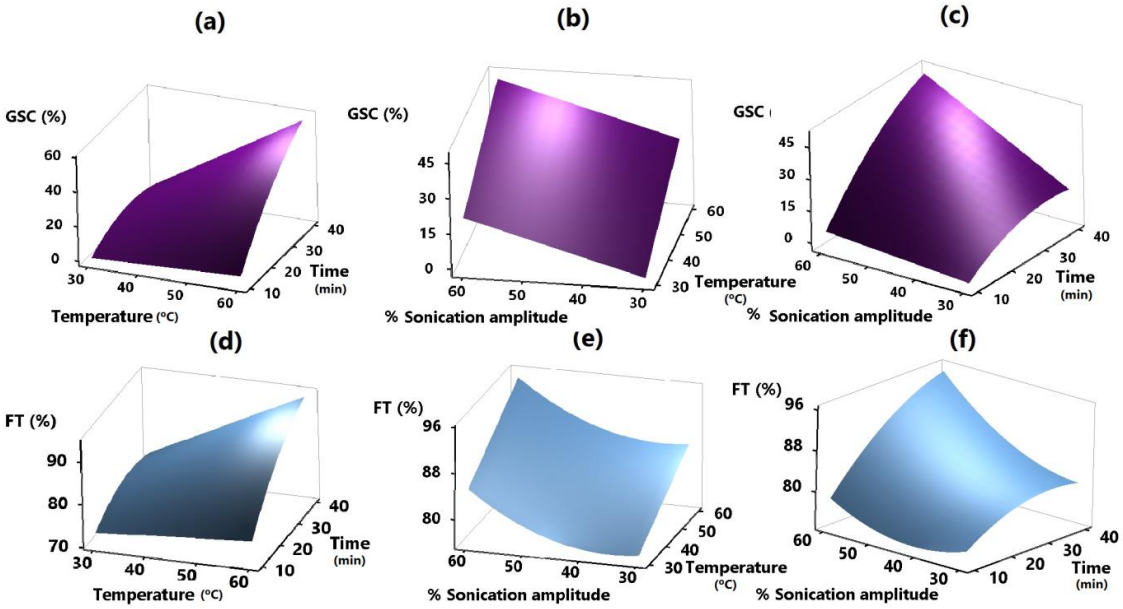

Figure 2.

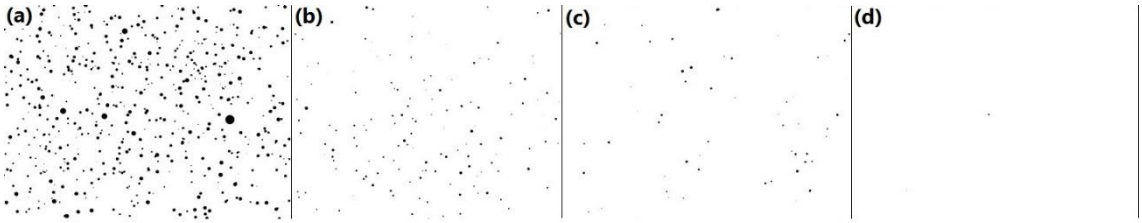

Figure 3.

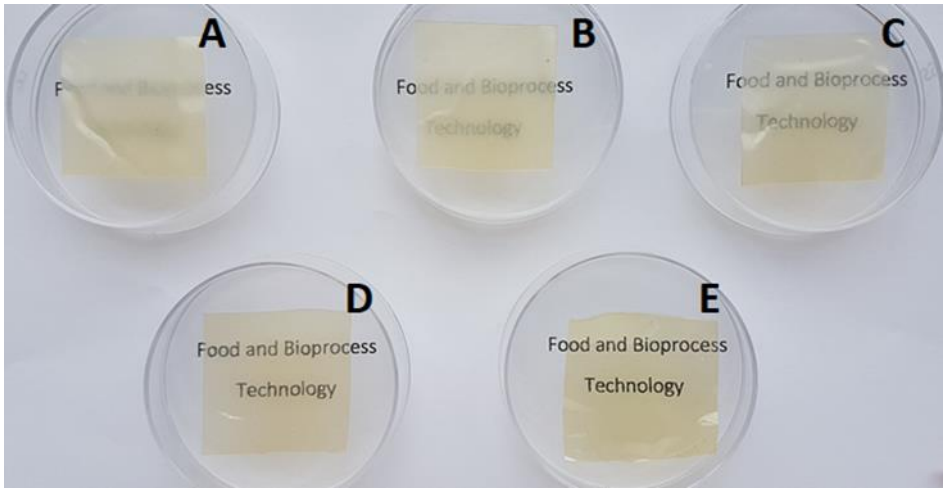

Figure 4.

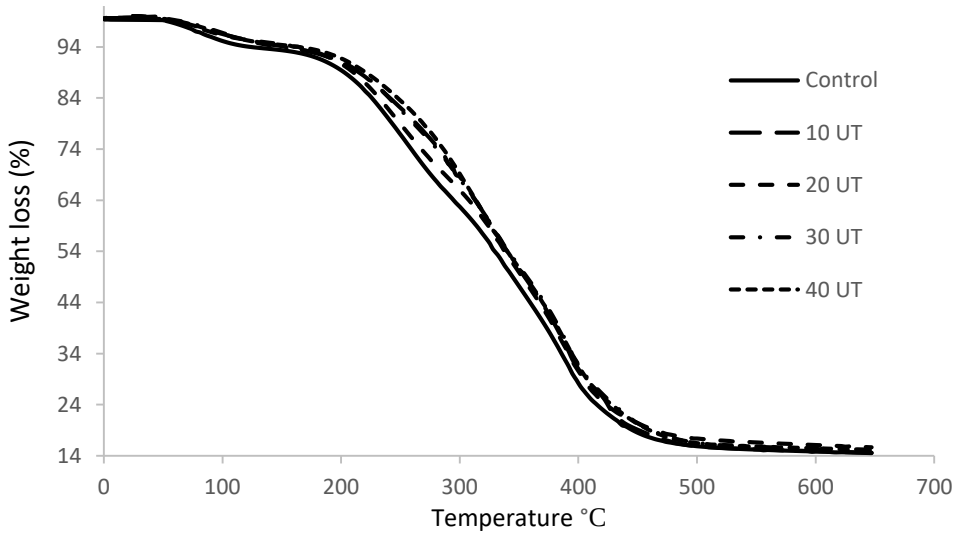

Figure 5.

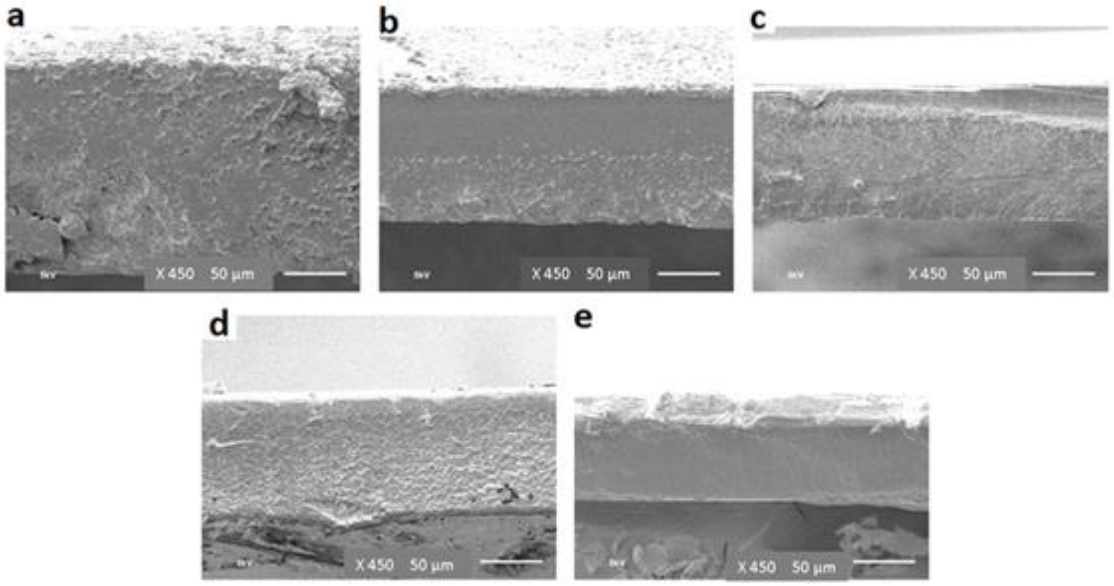

Table 1. Box-Behnken design matrix with the coded and uncoded values of the three independent variables and the two evaluated responses.

Run	**Independent variables**			**Dependent variables**		
	X_1 **Temperature (°C)**	**X_2** **Time (min)**	**X_3** **US amplitude (%)**	**Granule solution clarity (%)**	**Film transparency (%)**	**Film thickness (µm)**
1	30 (-1)	10 (-1)	45 (0)	0.3	72.0	119 ± 10[a]
2	60 (1)	10 (-1)	45 (0)	4.7	74.0	118 ± 18[a]
3	30 (-1)	25 (0)	30 (-1)	0.2	75.0	108 ± 15[a]
4	30 (-1)	40 (1)	45 (0)	5.0	77.0	115 ± 17[a]
5	45 (0)	10 (-1)	30 (-1)	2.0	78.0	110 ± 15[a]
6	45 (0)	10 (-1)	60 (1)	2.0	79.0	111 ± 10[a]
7	45 (0)	25 (0)	45 (0)	25.0	81.0	114 ± 18[a]

8	45 (0)	40 (1)	30 (-1)	18.3	82.0	117 ± 8[a]
9	45 (0)	25 (0)	45 (0)	22.0	84.0	115 ± 17[a]
10	45 (0)	25 (0)	45 (0)	23.0	84.0	116 ± 10[a]
11	60 (1)	25 (0)	30 (-1)	20.0	84.9	111 ± 9[a]
12	30 (-1)	25 (0)	60 (1)	21.2	85.0	118 ± 10[a]
13	45 (0)	40 (1)	60 (1)	48.5	94.4	105 ± 7[a]
14	60 (1)	40 (1)	45 (0)	57.0	94.2	106 ± 15[a]
15	60 (1)	25 (0)	60 (1)	52.0	96.0	110 ± 10[a]

Superscripts in the same experimental parameter indicate significant differences ($P < 0.05$).

Table 2. Analysis of variance of the regression models of the granule solution clarity and film transparency. Coefficients are expressed in coded form.

Source	**F**	**p-value**	**Estimated coefficient**	**Sum of squares**	**Degrees of freedom**	**Mean square**
	Granules solution clarity (%)					
Model	61.01	0.000		5024.49	6	837.41
Intercept			23.31			
$\mathbf{X_1}$	104.66	0.000	13.40	1436.48	1	1362.42
$\mathbf{X_2}$	130.71	0.000	14.98	1794.01	1	1436.48
$\mathbf{X_3}$	62.74	0.000	10.38	861.12	1	861.12
$\mathbf{X_2^2}$	10.09	0.013	-6.09	138.43	1	138.43
$\mathbf{X_{12}}$	41.27	0.000	11.90	566.44	1	566.44
$\mathbf{X_{23}}$	16.61	0.004	7.55	228.01	1	228.01
Lack of fit	7.51	0.122		105.14	6	17.52
$\mathbf{R^2}$	0.97					
$\mathbf{R^2_{adj}}$	0.96					
	Film transparency (%)					
Model	33.14	0.000		758.51	7	108.35
Intercept			82.43			
$\mathbf{X_1}$	65.61	0.000	5.01	200.80	1	200.80

X_2	81.13	0.000	5.57	248.31	1	248.31
X_3	48.47	0.000	4.30	148.35	1	148.35
X_2^2	9.04	0.020	-2.72	32.67	1	27.65
X_3^2	12.52	0.009	3.21	38.30	1	38.30
X_{12}	18.87	0.003	3.80	57.76	1	57.76
X_{23}	10.56	0.014	2.84	32.31	1	32.31
Lack of fit	1.03	0.560		15.42	5	3.08
R^2	0.97					
R^2_{adj}	0.94					

Table 3. Characterization of the particles contained in the granules solutions pre-treated with ultrasounds.

Sample (UT min)	**Dinamic Light Scattering**		**Fluorescence Microscopic Image Caption analysis[1]**	
	Polidispersity Index	Average Size (nm)	Particle population	Average Particle Area (μm^2)
0	0.4±0.01[a]	327±10[a]	528±60[a]	45.2±42.0
10	0.3±0.01[b]	219±12[b]	149±29[b]	18.1±14.1
20	0.3±0.03[b]	173±8[c]	57±8[c]	17.1±14.9
30	0.3±0.04[b]	154±12[c]	<2[d]	9.0 ±9.5
40	0.3±0.02[b]	138±2.5[d]	<2[d]	8.1±9.2

Values are expressed as means ± SD. Different letters in the same column indicate significant differences ($P < 0.05$). [1]: Parameters calculated from images presented in Figure 2.

Table 4. Film colour, thickness, moisture content (MC), water solubility (WS), water vapour permeability (WVP), puncture strength (PS) and puncture deformation (PD) of the films obtained after the ultrasound pre-treatment (UT).

Sample (UT min)	**Colour**				**Thickness (µm)**	**MC (%)**	**WS (%)**	**WVP (g·mm/ m^2·h·kPa)**	**PS (N/mm)**	**PD (%)**
	L*	a*	b*	ΔE control						
StD	97.12	-0.01	0.13							
Control	93.13±0.20[a]	1.5±0.17[a]	23.50±2.00[a]	0.0	132±5[a]	33±2[a]	16±0.2[a]	ND	9.0±2.0[a]	10±3.0[a]
10	92.96±0.21[a]	1.3±0.30[a]	25.65±2.80[a]	3.16	111±10[b]	27±1[b]	14±0.4[b]	1.78±0.1[a]	17.4±3.0[b]	39±8.0[b]
20	93.08±0.24[a]	1.6±0.40[a]	24.00±2.50[b]	0.51	111±9[b]	29±1.5[b]	14±0.7[b]	1.77±0.1[a]	21.2±3.5[b]	69±1.4[c]

30	93.39±0.32[a]	1.4±0.20[a]	23.57±3.00[a]	0.28	107±15[b]	28±0.5[b]	14±0.5[b]	1.78±0.1[a]	31.4±1.2[c]	100±3.3[d]
40	93.45±0.25[a]	1.3±0.12[a]	25.50±1.50[a]	2.35	105±7[b]	28±1[b]	14±0.5[b]	1.76±0.1[a]	31.6±2.5[c]	113±7.0[e]

Values are expressed as means ± SD. Different letters in the same column indicate significant differences ($P < 0.05$). ND: not determined